Bridge-free fabrication process for Al/AlO$_x$/Al Josephson junctions*

Ke Zhang(张珂)[1], Meng-Meng Li(李蒙蒙)[1], Qiang Liu(刘强)[1], Hai-Feng Yu(于海峰)[1,2,†], and Yang Yu(于扬)[1,2]

[1] National Laboratory of Solid State Microstructures, School of Physics, Nanjing University, Nanjing 210093, China

[2] Synergetic Innovation Center of Quantum Information & Quantum Physics, University of Science and Technology of China, Hefei 230026, China

(Received 7 March 2017; revised manuscript received 5 April 2017; published online 6 June 2017)

We fabricate different-sized Al/AlO$_x$/Al Josephson junctions by using a simple bridge-free technique, in which only single-layer E-beam resist polymethyl methacrylate (PMMA) is exposed at low accelerate voltage (below 30 kV) and the size of junction can be varied in a large range. Compared with the bridge technique, this fabrication process is very robust because it can avoid collapsing the bridge during fabrication. This makes the bridge-free technique more popular to meet different requirements for Josephson junction devices especially for superconducting quantum bits.

Keywords: Josephson junction, bridge-free technique, e-beam lithography, superconducting qubit

PACS: 85.25.Cp, 03.67.Lx, 85.25.Am **DOI:** 10.1088/1674-1056/26/7/078501

1. Introduction

As a key element of a superconducting quantum device, the Josephson junction has important applications in many areas of superconducting electronics such as the superconducting quantum interference device (SQUID),[1] rapid single flux quantum (RSFQ),[2] quantum bit (qubit),[3] and Josephson parameter amplifier (JPA).[4] Recently, with the rapid progress of superconducting quantum computing, aluminum based Josephson junctions attracted more and more attention due to their long decoherence time and simple fabrication process.[5–13] It is found that qubits consisting of aluminum junctions usually have much longer decoherence time than those made from other superconducting materials. Therefore, aluminum based junctions are widely used in qubit and JPAs[14,15] for realizing the quantum information process.

In order to obtain qubits with a long decoherence time, people usually use a simple fabrication process called the Dolan bridge technique,[16] which requires only one lithographic patterning step. By using bilayer E-beam resist, different exposure doses, and developing times, one can form a suspended bridge of E-beam resist. Then two layers of aluminum film are deposited with an electron beam evaporator from two angles. In order to obtain an Al/AlO$_x$/Al Josephson junction, people use an *in-situ* oxidation procedure before depositing the second aluminum layer to build a thin AlO$_x$ layer. Of course, the yield of this fabrication process crucially depends on the quality of suspended E-beam resist bridge. However, the E-beam resist bridge is usually fragile. It has a substantial probability of being damaged during the fabrication procedure. This limits the flexibility of the device design and fabrication process. Particularly, it is difficult to fabricate Josephson junctions with a large size (over 1 micrometer) by using this technique. Currently, large Josephson junctions are commonly used for making JPA which is an important device for realizing quantum non-demolition measurement of superconducting qubits. To solve these problems, Lecocq *et al.*[17] have developed a bridge-free technique by using a high accelerate voltage e-beam writer. Nevertheless, large area suspension of the upper layer E-beam resist still exists which is likely to collapse in the argon-milling process.

In this work, according to a single-layer E-beam resist technique for a sub-micron junction,[18] we develope a fabrication process for making aluminum junctions with various sizes. In our fabrication process, we use the most used E-beam resist polymethyl methacrylate (PMMA) and e-beam writer with low accelerate voltage. No suspended part of the E-beam resist is present and a single-layer resist on the line width control will be better than a double-layer resist. Therefore, we can use strong argon plasma etching to get rid of residual resist and native oxide layer in the fabrication process. Using this process, we fabricate transmon[19–22] qubits with junction sizes ranging from 0.04 μm^2 to 10 μm^2. The transmon qubits show reasonable decoherence time.

2. Fabrication and results

We use a 30-keV e-beam writer which is modified from a field emission scanning electron microscope (SEM) to perform e-beam lithography. The substrate for fabricating the device is a 0.5 mm-thick highresistivity silicon substrate. The e-beam resist used in this paper is MicroChemPMMA 950A5.

2.1. Bridge-free technique

Figures 1 and 2 show the principle of our Josephson junction fabrication process. After the substrate is cleaned, we

*Project supported by the National Key Research and Development Program of China (Grant No. 2016YFA0301802) and the National Natural Science Foundation of China (Grant Nos. 11474152, 91321310, 11274156, 11504165, and 61521001).

†Corresponding author. E-mail: hfyu@nju.edu.cn

© 2017 Chinese Physical Society and IOP Publishing Ltd

start the fabrication process by spinning one layer PMMA on the substrate. The thickness of PMMA is controlled at about 400 nm by adjusting the speed of the spinner. We bake PMMA coated substrate at 180 °C for 2 min. The wafer is subsequently exposed to e-beam with a dosage of 420 μC/cm^2–480 μC/cm^2 at 20 kV–30 kVe beam voltage. The sample is then developed in 1:3 MIBK/IMPA for 40 s and we obtain the complete pattern as shown in Fig. 1. Two schematic drawings (Figs. 1(a) and 1(b)) illustrate the shapes of PMMA pattern for different junction sizes. There are two perpendicular grooves which are able to form two leads of a junction after the film has been evaporated. The crosses define the area of junction. There is no suspended PMMA in each of these patterns. Therefore, we can use strong argon plasma etching to clean residual PMMA in the developed area. Then we will enter into the evaporation procedure. As shown in Fig. 1, we evaporate aluminum film along the directions of grooves. However, the evaporation angles with respect to the substrate plane, denoted as θ_1 and θ_2 respectively, are carefully designed to control the junction size and keep the leads single-layered as described later. Here we design a square junction with the same lead width. Therefore, we can simply use $\theta_1 = \theta_2 = \theta$. Figure 2 illustrates how the deposition forms the tunnel junction and leads. Figures 2(a)–2(d) show the film deposition in the junction area, corresponding to the cross section marked by the green dashed line in Fig. 1(a).

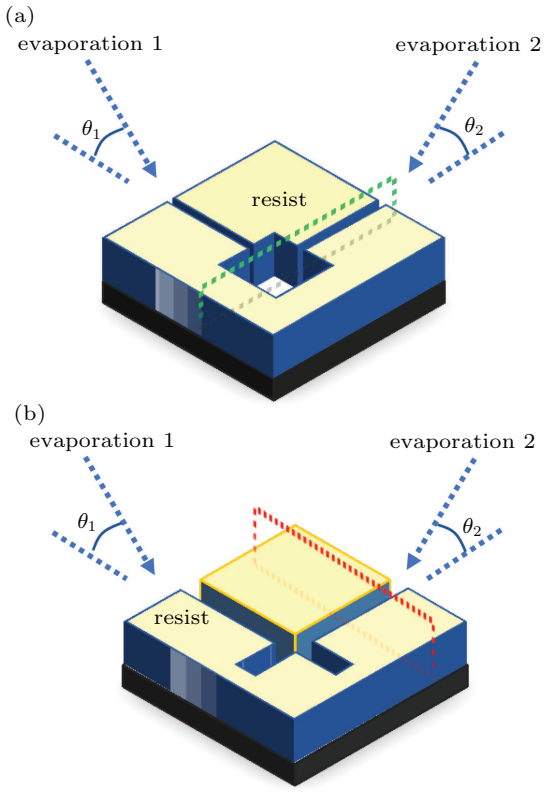


Fig. 1. (color online) Schematic diagrams of the PMMA pattern formed by our single-layer e-beam lithography process. The Josephson junctions are formed in the center of the cross after two-angle evaporation. (a) The pattern for the micrometer size junction. (b) The pattern for the nanometer size junction.

After oxidization, we rotate the sample holder 90 degrees and evaporate the second layer. The size of the junction is controlled by θ. However, θ is also limited by the evaporation of junction leads. Figures 2(e)–2(h) show the film depositions on the lead area, corresponding to the cross section marked by the red dash line in Fig. 1(b). It is obvious that θ has to be chosen carefully so that there is no film overlap on the substrate between two evaporations. We will discuss this quantitatively in the next section. Finally, we obtain the device after lifting off the aluminum on the PMMA as shown in Figs. 2(d) and 2(h).

2.2. Josephson junction size control

In order to fabricate a junction using this technique, we should follow the constrain $t/\tan\theta > l$, where t is the layer thickness and l is the width of the lead wires. When the above condition is satisfied, the aluminum film of neither evaporation 1 nor 2 can reach the bottom of the two perpendicular grooves. Only one angle evaporation will be deposited onto the substrate. Therefore, we are safe to keep the junction not shorted by the leads. Both evaporation angles are equally chosen to be 55°, and the thickness values of the first and second aluminum film are 30 nm and 80 nm respectively.

One of the crucial parameters of the Josephson junction is the size of the junction. As shown in Fig. 1, the area of the junction is mainly determined by the area of the intersection of the PMMA pattern. However, the thickness of PMMA and the evaporation angle are also relevant issues for junction size. For simplicity, we assume a square intersection with the side length L part when we fabricate the micrometer size junction, which is shown in Fig. 2(a). Because of the shadow effect of PMMA, the aluminum film will have small shifts in different evaporation directions, which makes the junction size smaller than the intersection part. The microscope image clearly shows this in Fig. 3(a). It is easy to calculate that the shift $s \approx t/\tan\theta$. Therefore, the actual junction size is $L - t/\tan\theta$, as shown in Fig. 2(d).

For a small junction with nanometer size, we usually pattern the junction width the same as that of the lead wire. Since two evaporations are along the lead directions, there is almost no shadow effect of PMMA. However, the aluminum film of the first evaporation will hang on one wall of the PMMA groove, blocking a small part of the second evaporation. We assume that the aluminum deposited on the wall of the PMMA has a rectangular cross section as shown in Fig. 2(f). For this geometry, we obtain the undercut $W_1 \approx t_1/\tan\theta$, where t_1 is the thickness of the first aluminum layer. Therefore, the actual width of lead W is about $l - t_1/\tan\theta$. Considering that only one layer t will be blocked, we obtain that the area of junction is about $l(l - t_1/\tan\theta)$. In Fig. 3, we show the SEM image, where the shadow effect can be clearly observed for large junctions.

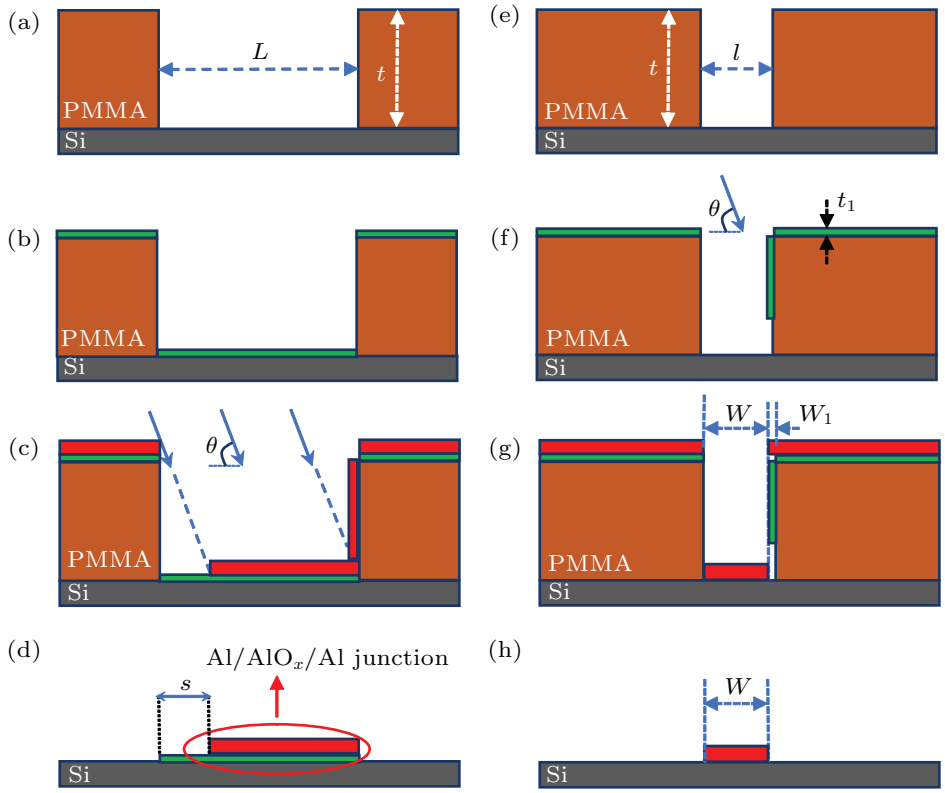


Fig. 2. (color online) (a)–(d) Film evaporation in the junction area (the cross section marked with the blue dashed line in Fig. 1). (e)–(h) Film evaporations at the lead area (the cross section marked with the red dashed line in Fig. 1). The oxidation process between two evaporations is not shown. (a), (e) Before evaporation. The sizes of the groove are L and l, respectively. (b), (f) Evaporations of the junction bottom layer with an angle θ with respect to the substrate plane. (c), (g) Evaporation of the top aluminum layer after rotating the sample holder 90 degrees with an angle θ with respect to the substrate plane. (d), (h) Final view of our junction and lead.

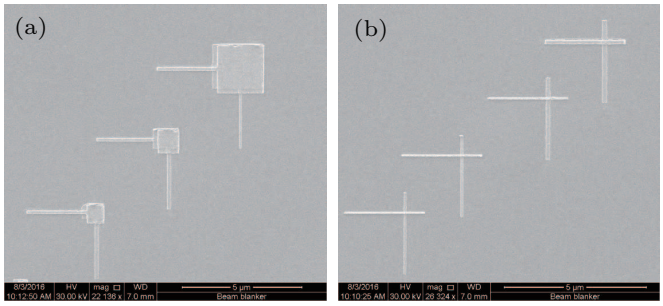


Fig. 3. Scanning electron microscope (SEM) image for (a) micrometer size junctions, showing that the defined and (actual) areas of large junctions from left to right are 800×800 (680×590), 1000×1000 (890×800) and 2000×2000 (1930×1820) nm^2, and for (b) nanometer size junctions, showing that the defined and (actual) areas of small junctions from left to right are 80×80 (96×72), 100×100 (104×75), 120×120 (160×80), and 200×200 (214×187) nm^2.

2.3. Fabrication and calibration of superconducting qubits

By using this technique, we fabricate three-dimensional (3D) transmon qubits[21] on silicon wafer. The size of junction is about 190×170 nm^2. Then we calibrate the quantum dynamics of the 3D transmon qubits. The qubits are cooled in a cryogenfree dilution refrigerator to a base temperature of about 20 mK. We use the "high power readout"[22] scheme to readout the transmon state. We measure Rabi oscillations and the energy relaxation time of the qubits. The typical Rabi oscillations and energy relaxation are shown in Fig. 4. The qubit frequency is about 8.3877 GHz. The energy relaxation time is about 2.1 μs, which is comparable to that of our qubits fabricated with former procedures.

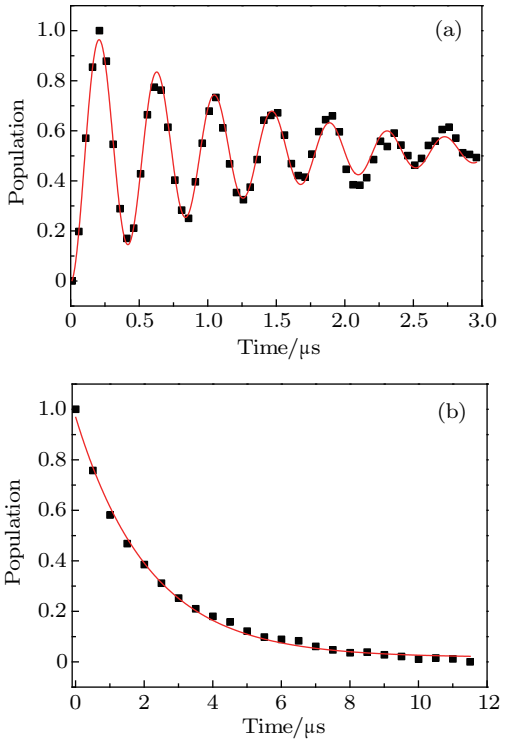


Fig. 4. (color online) (a) Rabi oscillations, and (b) relaxation time of 3D transmon sample fabricated with the bridge-free technique.

3. Conclusions and perspectives

By using the one layer resist PMMA bridge-free technique, we fabricate Al/AlO_x/Al Josephson junctions. This technique can be used to fabricate junctions with diverse sizes ranging from 0.04 μm^2 to 10 μm^2. The property of 3D transmon qubit fabricated with this technique indicates that our technique is valid, proving the potential of this simple process in superconducting quantum computation.

Acknowledgment

All the microfabrication processes were done in the Microfabrication Center of the National Laboratory of Solid State of Microstructures. We thank Kai Qiu, Chunyu Huang, and other staff for their help.

References

[1] Clarke J and Braginski A I 2004 *The SQUID Handbook* (Weinhein: Wiley-VCH)
[2] Mukhanov O A and Semenov V K 1985 Preprint No. 9/1985, Dept. of Physics, Moscow State University, Moscow, Russia
[3] You J Q and Nori F 2005 *Physics Today* **58** 42
[4] Yamamoto T, Inomata K, Watanabe M, Matsuba K, Miyazaki T, Oliver W D, Nakamura Y and Tsai J S 2008 *Appl. Phys. Lett.* **93** 042510
[5] Wallraff A, Schuster D I, Blais A, Frunzio L, Huang R S, Majer J, Kumar S, Girvin S M and Schoelkopf R J 2004 *Nature* **431** 162
[6] Barends R, Kelly J, Megrant A, Sank D, Jeffrey E, Chen Y, Yin Y, Chiaro B, Mutus J, Neill C, O'Malley P, Roushan P, Wenner J, White T C, Cleland A N and Martinis J M 2013 *Phys. Rev. Lett.* **111** 080502
[7] Chow J M, Córcoles A D, Gambetta J M, Rigetti C, Johnson B R, Smolin J A, Rozen J R, Keefe G A, Rothwell M B, Ketchen M B and Steffen M 2011 *Phys. Rev. Lett.* **107** 080502
[8] Reed M D, DiCarlo L, Johnson B R, Sun L, Schuster D I, Frunzio L and Schoelkopf R J 2011 *Phys. Rev. Lett.* **105** 173601
[9] Jin X Y, Kamal A, Sears A P, Gudmundsen T, Hover D, Miloshi J, Slattery R, Yan F, Yoder J, Orlando T P, Gustavsson S and Oliver W D 2015 *Phys. Rev. Lett.* **114** 240501
[10] Weber S J, Chantasri A, Dressel J, Jordan A N, Murch K W and Siddiqi I 2014 *Nature* **511** 570
[11] de Lange G, Ristè D, Tiggelman M J, Eichler C, Tornberg L, Johansson G, Wallraff A, Schouten R N and DiCarlo L 2014 *Phys. Rev. Lett.* **112** 080501
[12] Eichler C, Lang C, Fink J M, Govenius J, Filipp S and Wallraff A 2008 *Phys. Rev. Lett.* **109** 240501
[13] Liu Y H, Lan D, Tan X S, Zhao J, Zhao P, Li M, Zhang K, Dai K Z, Li Z Y, Liu Q, Huang S D, Xue G M, Xu P, Yu H F, Zhu S L and Yu Y 2015 *Appl. Phys. Lett.* **107** 202601
[14] Castellanos-Beltran M A, Irwin K D, Hilton G C, Vale L R and Lehnert K W 2008 *Nat. Phys.* **4** 929
[15] Bergeal N, Schackert F, Metcalfe M, Vijay R, Manucharyan V E, Frunzio L, Prober D E, Schoelkopf R J, Girvin S M and Devoret M H 2010 *Nature* **465** 64
[16] Dolan G J 1977 *Appl. Phys. Lett.* **31** 337
[17] Lecocq F, Pop I M, Peng Z H, Matei I, Crozes T, Fournier T, Naud C, Guichard W and Buisson O 2011 *Nanotechnology* **22** 315302
[18] Potts A, Parker G J, Baumberg J J and de P A J 2001 *IEE Proceedings - Science Measurement and Technology* **148** 225
[19] Koch J, Yu T M, Gambetta J, Houck A A, Schuster D I, Majer J, Blais A, Devoret M H, Girvin S M and Schoelkopf R J 2007 *Phys. Rev. A* **76** 042319
[20] Schreier J A, Houck A A, Koch J, Schuster D I, Johnson B R, Chow J M, Gambetta J M, Majer J, Frunzio L, Devoret M H, Girvin S M and Schoelkopf R J 2008 *Phys. Rev. B* **77** 180502
[21] Paik H, Schuster D I, Bishop L S, Kirchmair G, Catelani G, Sears A P, Johnson B R, Reagor M J, Frunzio L, Glazman L I, GirvinS M, Devoret M H and Schoelkopf R J 2011 *Phys. Rev. Lett.* **107** 240501
[22] Reed M D, DiCarlo L, Johnson B R, Sun L, Schuster D I, Frunzio L and Schoelkopf R J 2010 *Phys. Rev. Lett.* **105** 173601